

ACCURACY ANALYSIS OF CIRCULAR IMAGE BLOCK ADJUSTMENT

Jussi Heikkinen

Institute of Photogrammetry and Remote Sensing
Helsinki University of Technology, P.O.Box 1200, FIN-02015 Espoo, Finland
Jussi.Heikkinen@hut.fi

Commission V, WG V/1

KEY WORDS: Photogrammetry, Adjustment, Bundle, Block, Estimation, Close Range

ABSTRACT:

Circular image block method has been developed for special photogrammetric close-range cases. Circular image block approach is not meant to substitute the current close-range photogrammetric network design methods, but simply to provide a new tool to be used with current methods. This method is beneficial in conditions where the traditional approach in network design problem meets its limitations; in cases when the photogrammetric network and camera stations cannot be around the object, but the imaging has to be done inside the object space. A new mathematical model had to be designed for the spherical imaging. However, this method is based on block of individual bundles of rays unlike the panoramic imaging. In this paper the method in real measuring tasks is evaluated in terms of accuracy and robustness. In order to evaluate the performance, a practical test was accomplished by measuring an object point set with varying object distances. Results are compared with reference data as well as with results of the simulated tests with similar test parameters. Discussion is given about the problem of initial values and the suitability of the method in an object reconstruction project.

1 INTRODUCTION

The circular image block method is especially designed for measurements of fairly large objects and for special photogrammetric close-range cases. This approach is beneficial in special conditions where the traditional approach in network design (Fraser, 1989) problem meets its limitations; e.g. when visibility is some how compromised like with very complex object structures. The only solution to this problem is that imaging has to be done inside the object space, not around the object. This often leads to construct a set of smaller image sub blocks, which have to be transformed into a common coordinate system afterwards. The reason why all image measurements are not handled in same adjustment is that usually the network geometry in such cases is too weak and common bundle adjustment would lead to deformations in object model. Rigid conformal transformation is usually used for transferring the sub models into common coordinate system. Unfortunately, this kind of approach generates quite a number of sub blocks and some image management system is then required to manage the whole measuring project. Also, more effort has to be put in search of correspondent object features for coordinate transformation purpose. These numerous sub blocks are difficult to handle in the same project and their orientation can be quite arbitrary in object space.

Circular image block method will reduce the number of sub blocks needed in photogrammetric measuring tasks, as well provide a better geometry in photogrammetric network. Image block design called here 'Circular Image Blocks' is a block of images who share common properties. All camera positions in a block have the same property that their projection centres lie on the same plane in

object space. Another relation between projection centres is that a single circle on that plane can be drawn which goes through all the projection centres and orientation of camera is static respect to the trajectory of this circle. The final assumption is that successive images have overlap between them and overlap also exists between the first and last image in the block.

These are quite strict assumptions, but in practice, it is quite simple actually to fulfill the conditions by using a rod with certain length for the purpose. The camera is fixed in one end of the rod and the other end will be fixed to some stationary point. The rotation of the rod is only around this stationary point on a specific plane. This yields to an image block covering the scenery of full 360° deg from one point. The image measurements will be the correspondent image points on successive images. The weakness of such block is that all successive camera positions have divergent orientations. In order to overcome this problem two co-centric image blocks are recommended to be constructed and adjustment of both blocks should be done simultaneously including estimation of angular difference between the blocks. The camera is fixed perpendicularly to the rod. In the first block in direction of $+90^\circ$ and in the second block -90° . This way we can find camera positions with converging viewing directions at most two times the length of the rod apart from each other, see Figure 1.

The whole idea is that we can bind multiple images, bundles of rays, into two image blocks and substitute their orientation parameter with fewer block parameters. As we are handling a constrained image block we might introduce few constrain equations into adjustment process. Our approach is to reparametrize the image parameters in the image block in order to fulfill the requirements for the

2 SIMULATION

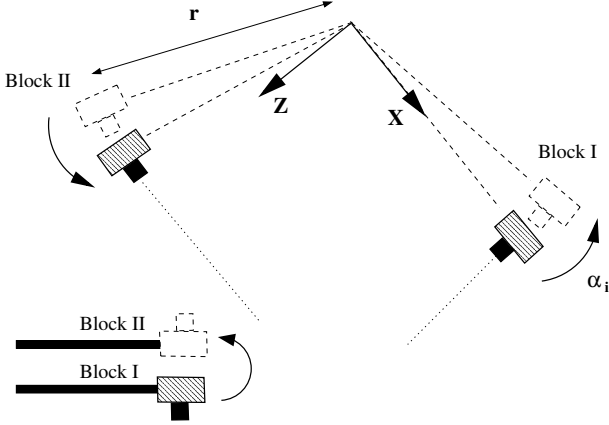


Figure 1: Circular image block imaging constellation. Between first and second block creation the camera will be turned into opposite direction.

block. We have here a free net type estimation problem. As we have no exterior co-ordinate information, we create a co-ordinate system of our own. In order to solve insufficient datum problem we might minimize the sum of variance-covariances of the parameters, which is a common approach. Another approach, which we have used, is to fix sufficient number of parameters. The rotation of the camera is supposed to be done on xz -plane. So all camera poses have their y -coordinate fixed to zero. The x -axis is fixed into direction of the first camera pose of the first image block and origin of the co-ordinate system is in the centre of rotation. All other camera pose co-ordinates are expressed in polar-co-ordinates.

$$\begin{cases} X_i = r \cdot \cos \alpha_i \\ Y_i = \text{constant} \\ Z_i = r \cdot \sin \alpha_i \end{cases} \quad (1)$$

The rotation of the camera in each camera pose respect to this local co-ordinate system is also dependent of this one parameter α_i unique for each camera pose. Also, it is dependent of the orientation of first camera pose in image block.

$$R_{\omega_i, \phi_i, \kappa_i} = R_{\omega_0, \phi_0, \kappa_0} \cdot R_{\alpha_i} \quad (2)$$

Here rotation matrices R are assumed to be 3×3 orthonormal rotation matrices, where rotations are supposed to be done subsequently. For each image block we have four common parameters $\omega_0, \phi_0, \kappa_0$ and r and for each camera pose we only have one unique parameter α_i . Only for first camera pose of the first image block we have fixed $\alpha_0 = 0$. This way we can express the block with fewer parameters in more compact form and benefit from overdetermination in our measurements. By adding at least one distance measurement we can also have our image block in a right scale. More thorough representation of the method can be found in (Heikkinen, 1998; Heikkinen, 2000; Heikkinen, 2002).

The method has been tested previously with simulation. The purpose of simulation was to verify the correctness of the mathematical model of the system. Finding the power of the method was also one purpose of the simulations.

Measuring system of the circular image block resembles a geometry of stereo imaging, so it is natural to test the same parameters which are most important in a stereo pair imaging system. Namely, the length of the baseline; here the length of the radius; and the precision of the image measurements. However, this imaging system cannot be regarded as a group of stereo pairs. Each photo in an image block is considered as an individual image ray bundle, whose pose and orientation are bounded by common block parameters. In this sense the number of photos included in a image block also has significance on the measuring accuracy. Therefore finding the effect of different number of photos in image block was one of the goals of simulation tests.

In all simulations the arrangements were similar; the same object point group; the same camera orientation for the first camera pose in a block $R_{0,0,0}$ and $R_{0,180,0}$; the same camera model (1024x1280pix; $c=1400$ pix). The object point group was generated by random point generation. Only some restrictions were given how far from the center points were allowed to align. Image observations were generated by back-projecting the object points onto image plane according to camera orientation information. In order to simulate the accuracy of image observations random noise was generated and added to the image points. So the varying test parameters were; the level of random noise added on image observations, the length of the radius and the number of photos included in image block. Only one of the test parameters was alternated in one simulation. In each simulation 100 test runs were accomplished and random noise was added to image observations individually between each test run to achieve reliable test results. The results of a simulation of varying length of radius in the imaging constellation are represented in Figure 2. The number of photos in one block was 30 and noise level added into the image observation was 0.2 pixels. More information of simulation results can be found in previous publications (Heikkinen, 2001; Heikkinen, 2002).

The simulation environment was also used on testing the limits of the goodness of initial values. The parameter values were slightly changed from their correct values and only one parameter was alternated at a time. The test was first accomplished without noise and then with only a small amount of noise added to the image observation. The orientation angles of the first camera were more sensitive to incorrectness of initial values than α -angle of each photo or length of radius r . For ω, ϕ, κ -angles the initial values were required to be better than 3–5 deg in order to meet convergence. For α -angles 5 deg was generally good enough and for length of radius r initial value $\pm 5cm$ was acceptable.

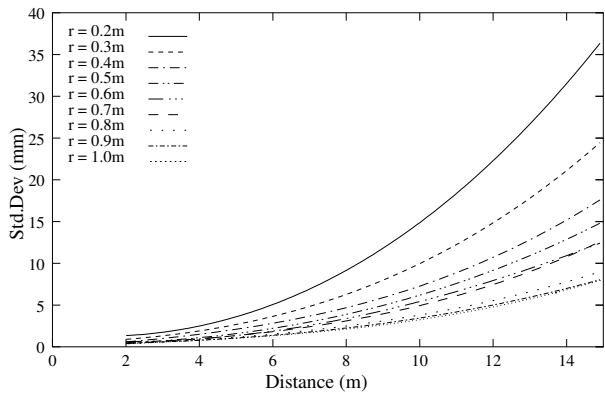


Figure 2: The object point co-ordinate deviation respect to object distance. Each curve illustrates the imaging configuration with certain length of radius.

3 ARRANGEMENT OF EXPERIMENT

In the first field demonstration the arrangements of the imaging constellation were as similar as possible to the simulation environment. Approximately 30 photos were taken per image block and camera was nearly perpendicular to the supporting rod. The effort was made to take photos with as equal-angled as possible. Despite of that, received initial values for block parameters were not good enough and there were real difficulties to get iteration converge. Finally, the image block estimation could be computed, but residuals were not acceptable. Systematic errors in residuals were clearly visible and most of the residuals were vertically directed. This indicated that either camera calibration was not correct or the requirement of projection centers lying on the same plane was violated. The latter was suspected and therefore a new more controllable imaging system was designed.

3.1 Motorized imaging system

In the first experiment, the revolving rod was attached to tripod with a rotary actuator without ball bearing and no precise scale was present to assist in evaluating the approximate rotation of the rod between shots. To prevent abnormality in height of the projection centers during imaging and in order to receive better initial values, a ball bearing supplied rotation system was designed and assembled. Better rotation control was achieved by supplying the system with a worm gear and a step motor (Figure 3). Step motor was controlled by computer to rotate the camera with equal-angled steps. Camera was also triggered automatically under computer control.

This type of system design provided fully automatic imaging without human intervention. Camera setups were fixed into constant focus (infinity) and the aperture was also predetermined according to setup values used in previous camera calibration.

3.2 Experiment in real conditions

Next experiment was run in interior space in an entrance hall, which consisted of a corridor, two round columns and

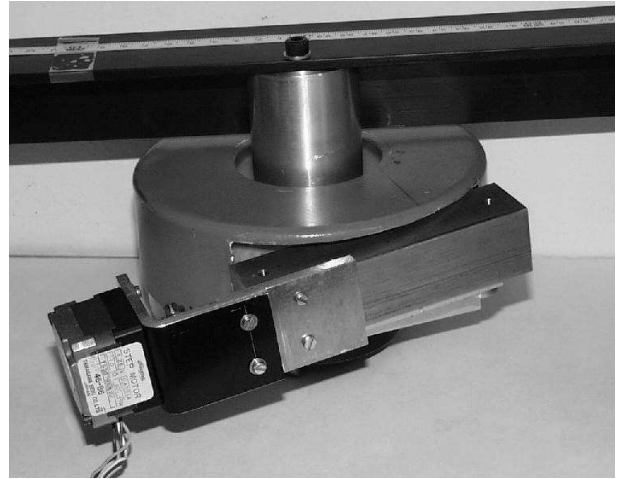


Figure 3: Step motor driven imaging system.

a staircase (Figure 4). So the conditions were such that one could meet when carrying out a typical measurement task in interior space; blind angles, small angles between wall surface and viewing angle plus varying illumination. The maximum distance inside the area was approximately 40 meters.



Figure 4: The entrance hall where the experiment took place.

The idea was to evaluate the system accuracy from the single imaging station. For the reference datum the targeted points were measured by a tachymeter. Tachymeter measurements were based on simple horizontal/vertical angles and a distance. Prism used in measurements was a typical big prism used in field work. So no special instrumentation was used. In tachymeter measurements there occurred some difficulties to get prism detected by tachymeter. This caused that in the final accuracy analysis it was sometimes hard to evaluate, which discrepancies between photogrammetric data and reference data are a consequence of inaccuracy of photogrammetric data and which is due to unreliability of the reference data.

The imaging was made at the same spot as tachymeter measurements. Rotation center of imaging differed only few millimeters from the tachymeter coordinate system. This was verified afterwards with a coordinate system conversion. Imaging was accomplished with computer con-

trolled system with 32 photos per image block and camera was attached to supporting rod approximately 45cm apart from the rotation center with perpendicular viewing angle. The camera settings were fixed to same focus and aperture values as used in camera calibration. The exposure time was allowed to be determined by automatic function of the camera. The camera used in experiment was an Olympus E-10 (1680x2240pix c=2350pix) digital still camera. The imaging was carried out under artificial illumination conditions and there was no control how fluorescent lamps took place on image in an individual shot. For this reason some images were over exposed and some under exposed. Still, targets were able to be measured on images reasonably well. The scale bar with length of $2m$ provided the scale for the 3-D measurements.

The targeted points were measured on images by applying image correlation and image LSQ-techniques. On chosen source image template was extracted in size selected by the operator. The selection was made in sub-pixel accuracy. The best position of template on next image on sequence was resolved with largest cross-correlation inside the search area. The final position was then estimated with LSQ-estimation with sub-pixel accuracy. This resolved best position of the template on target image was then used to extract a new template on this image for matching on next image. So the template image and target image were always from subsequent images. This way we could be sure that viewing angle on these camera poses did not differ much. This semiautomatic matching continued until the point was out of sight or occluded. For matching stopping criteria some limit correlation value was assigned. In order to get same target points measured on the second block, the previously measured image points were used as templates in matching on the image of the second block. The selection and locating the good initial position on second block image was given by operator. The best image pair for this point transfer was evaluated according to initial orientation. Images with nearly identical orientation angles were preferred.

4 ACCURACY ANALYSIS

The initial values for α -angle parameters were received from computer controlled imaging system as an output. The initial values for radius r was measured by simple tape measure and camera was supposed to be attached to rod with orientation angles $\omega_1 = 0$, $\phi_1 = 0$ and $\kappa_1 = 0$ for the first block and $\omega_2 = 0$, $\phi_2 = 180$ and $\kappa_2 = 0$ for the second.

At the first stage camera calibration values were fixed. After an adjustment the size of residuals and standard deviation of unit weight were reasonable. Investigating the residuals more closely a clear systematic error was visible. On some images main direction of residuals was upward and on other images it was downward. At first, the inconsistency was suspected to be result of incorrect calibration values. Therefore, the next step was to take calibration parameters with in the adjustment. Although as a result of this action the size of residuals and standard deviation of

unit weight were substantially reduced, still on some images the similar systematic pattern was present. Especially on images where object point distance was larger. In order to observe results as 3-D point coordinates, photogrammetric measurements were transformed to same coordinate system with reference data with rigid 3-D transformation. Big discrepancy between point sets was evident, especially on points far away. The previous residual inspection indicated clear inconsistency in image information. So this kind of occurrence of differences was quite presumable.

Based on these adjustment computations a suspicion of camera after all not lying on one plane during imaging arose. More support for this theory came when discovering that similar phenomenon had been reported to appear with panoramic cameras (Parian and Grün, 2004). The “tumbling” motion was explained to be caused by an incomplete shape of ball bearing and the contacting surfaces. To get evidence of existence of this type of phenomenon, the combined image block was calculated as photogrammetric free network adjustment. In this adjustment the number of parameters was $n * 6 + m * 3$ where n denotes the total number of images in block and m the number of object points. The convergence was achieved after few hundred iteration rounds and size of residuals and sigma was essentially smaller than on previous attempts. We have to remember now that this image block was free of constraints between camera orientation parameters. So parameter values were free to adjust according to image information. Looking more closely at precision values and reliability of parameters it was obvious that system was not capable of finding parameter values reliably with such an imaging geometry and there was clear evidence of over-parametrization. However, by examining the height values of projection centers we can notice clear fluctuation from the nominal height (Figure 5).

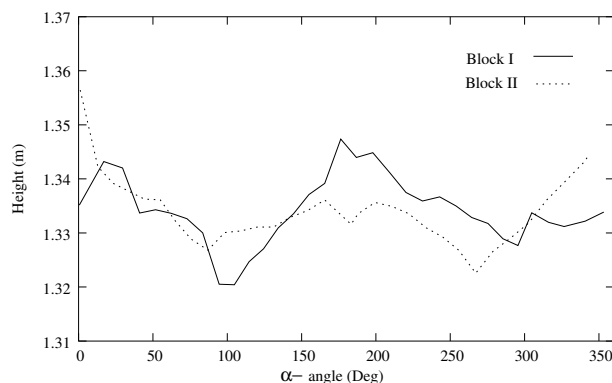


Figure 5: The fluctuation of projection center y-coordinates after free net adjustment. Values are depicted according to two separate image blocks.

This was convincing enough to improve the mathematical model to include also this kind of variation on camera height values. So an additional parameter θ was added to the model to describe the height difference from the nominal plane of rotation on each camera pose. The number of parameters was increased by $n - 1$ from the original set of parameters in Equations 1 and 2. Only first camera of the first block was supposed to have a fixed θ -value defining the

nominal plane. The total number of parameters was nearly doubled, but still it was only a fraction of equivalent number of a free net model. The new model can be represented as following.

$$\begin{cases} X_i = r \cdot \cos \alpha_i \cdot \cos \theta_i \\ Y_i = r \cdot \sin \theta_i \\ Z_i = r \cdot \sin \alpha_i \cdot \cos \theta_i \end{cases} \quad (3)$$

Also a change was made how the rotation matrix of individual camera pose is derived from block parameter angles.

$$R_{\omega_i, \phi_i, \kappa_i} = R_{\omega_0, \phi_0, \kappa_0} \cdot R_{\alpha_i, \theta_i} \quad (4)$$

The block adjustment was recomputed with the new model. Now the systematic pattern was essentially reduced. Similar illustration of projection center height fluctuation was depicted as with free net solution (Figure 6). From the same figure it can clearly be seen that there is approximately a 6mm height difference between image blocks, otherwise fluctuation inside one block is rather small in size of $1 - 2\text{mm}$.

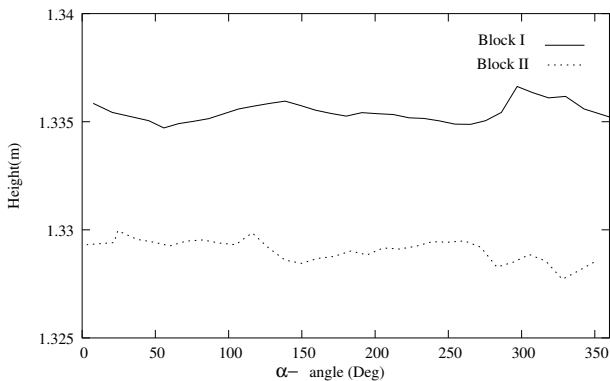


Figure 6: The fluctuation of projection center y-coordinates after adjustment with refined estimation model. Values are depicted according to two separate image blocks respect to α -angle.

The shift on y-coordinates of the projection centers between two blocks might have happened when camera was turned around in opposite direction in order to create the second block.

4.1 Accuracy assessment

In order to compare photogrammetric data with reference data the rigid 3D transformation between data sets was calculated. The length of point differences represents the absolute coordinate difference between data sets including inaccuracies of both measuring methods and the coordinate transformation (Figure 7). The point differences near the origin are more due to unsuitability of tachymeter measuring in short distances. Whereas the tachymeter coordinates of points far off are more reliable, the differences between data sets there are more due to limitation of photogrammetric methods. The second order curve (depicted in Figure 7)

was fitted into the data set of point differences. It can be compared with equivalent representation of simulated data in Figure 2. Although, it has to be remembered that the camera model and imaging configuration were not entirely equivalent.

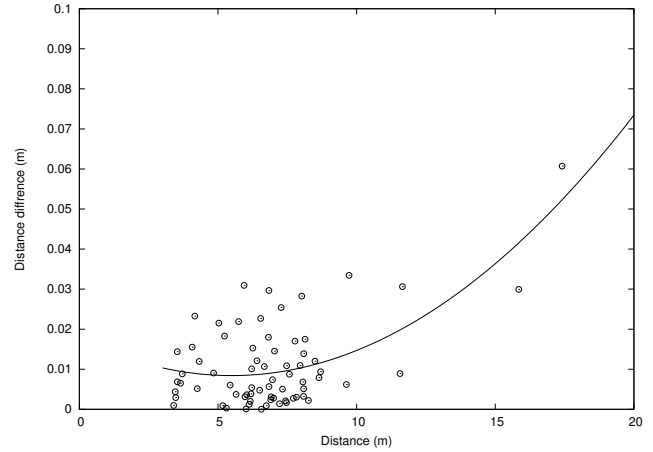


Figure 7: The length of point differences respect to object distance.

As mentioned before, the tachymeter data cannot be treated totally free of errors. More representative depiction of how consistent the photogrammetric data set is, or is not, with tachymeter data, can be seen in Figure 8. For this representation, all possible combinations of line segments inside the data set were calculated and corresponding lengths of lines in both data sets were compared respect to nominal values of the line lengths. In Figure 8 the second order curve depicts the prevalent tendency of differences respect to line lengths. The variation of differences in length is presumably due to distance of the point pair from origin. More far off the point pair locates from the origin, more inaccurate the point determination is. Based on this assumption it is obvious that longer the line segment is, more probable it is that at least one of the points will locate farther off. Therefore the variation with longer lines is larger than with shorter ones. In Figure 8 it is essential to notice that with lines about 10m long the difference is below 10mm in most cases. This tells about reasonable consistency with data sets.

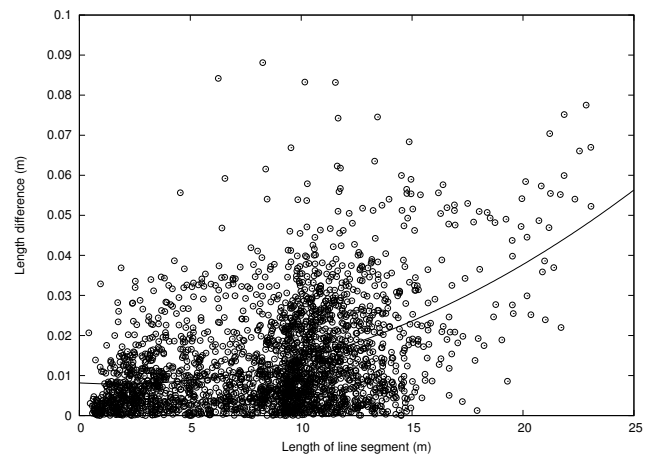


Figure 8: Comparison of data set point pairwise. The difference is depicted respect to length of line segments.

5 CONCLUSIONS

In this paper the refined mathematical model has been represented, which also encompasses possible deviation from the ideal model of imaging in practice. Also self-calibration technique has been applied in the estimation model on the final stage. Acquiring initial values for parameters is quite a straight forward procedure, which can partly be computerized with simple instrumentation. Some attention has to be paid to their correctness though. The method has been tested in real close-range measuring conditions without any optimization. Despite some unreliability in the reference data the accuracy with this method can be estimated to be better or at least the same as with equivalent stereo pair measurements. When the object space to be measured is up to 20 – 30m the achieved accuracy of 0.01 – 0.02m is quite adequate for large variety of applications.

However, in order to reveal the real power of this method, further research work has to be done and more specific tests have to be arranged where imaging and measuring conditions are not the limiting factors. The presented method is designed to be used for measuring surrounding object space from the single point of location. However, more than one such camera stations can be combined to achieve more precise and geometrically improved constellation in terms of measuring accuracy.

REFERENCES

- Fraser, C., 1989. Optimatization of networks in non-topographic photogrammetry. ASPRS, Falls Church, Virginia U.S.A., pp. 95–106.
- Heikkinen, J., 1998. Video based 3d modeling. In: Real-Time Imaging and Dynamic Analysis, Vol. XXXII, Part 5, ISPRS, Hakodate, Japan, pp. 712–716.
- Heikkinen, J., 2000. Circular image block measurements. In: XIX ISPRS Congress, Vol. XXXIII Part B5/1, ISPRS, Amsterdam, Netherlands, pp. 358–365.
- Heikkinen, J., 2001. Video measurements for forest inventory. In: S. E. Hakim and A. Grün (eds), Videometrics and Optical Methods for 3D Shape Measurements, Vol. 4309, SPIE, San Jose, CA U.S.A., pp. 93–100.
- Heikkinen, J., 2002. Performance of circular image blocks in close-range photogrammetry. In: Close-Range Imaging, Long-Range Vision, Vol. XXXIV Part 5, ISPRS, Corfu, Greece, pp. 39–41.
- Parian, A. J. and Grün, A., 2004. A refined sensor model for panoramic cameras. In: H.-G. Maas and D. Schneider (eds), Panoramic Photogrammetry Workshop, Vol. XXXIV Part 5/W16, ISPRS, Dresden, Germany.